



## Article

# Insulin protects against type 1 diabetes mellitus-induced ultrastructural abnormalities of pancreatic islet microcirculation

Bing Wang<sup>1,†</sup>, Xu Zhang<sup>2,†</sup>, Mingming Liu<sup>1,3,\*</sup>, Yuan Li<sup>1</sup>, Jian Zhang<sup>1,3</sup>, Ailing Li<sup>1</sup>, Honggang Zhang<sup>1,\*</sup>, and Ruijuan Xiu<sup>1</sup>

<sup>1</sup>Institute of Microcirculation, Chinese Academy of Medical Sciences & Peking Union Medical College, Beijing, 100005, China, <sup>2</sup>Laboratory of Electron Microscopy, Pathology Center, Peking University First Hospital, Beijing, 100034, China, and <sup>3</sup>Diabetes Research Center, Chinese Academy of Medical Science, Beijing 100005, China

\*To whom correspondence should be addressed. E-mail: mingmingliu@imc.pumc.edu.cn

†These authors contributed equally to this study.

Received 16 February 2020; Revised 6 July 2020; Accepted 6 July 2020

## Abstract

Pancreatic islet microcirculation, consisting of pancreatic islet microvascular endothelial cells (IMECs) and pericytes (IMPCs), provides crucial support for the physiological function of pancreatic islet. Emerging evidence suggests that pancreatic islet microcirculation is impaired in type 1 diabetes mellitus (T1DM). Here, we investigated the potential ultrastructural protective effects of insulin against streptozotocin (STZ)-induced ultrastructural abnormalities of the pancreatic islet microcirculation in T1DM mouse model. For this purpose, pancreatic tissues were collected from control, STZ-induced T1DM and insulin-treated mice, and a pancreatic IMECs cell line (MS1) was cultured under control, 35 mM glucose with or without  $10^{-8}$  M insulin conditions. Transmission and scanning electron microscopies were employed to evaluate the ultrastructure of the pancreatic islet microcirculation. We observed ultrastructural damage to IMECs and IMPCs in the type 1 diabetic group, as demonstrated by destruction of the cytoplasmic membrane and organelles (mainly mitochondria), and this damage was substantially reversed by insulin treatment. Furthermore, insulin inhibited collagenous fiber proliferation and alleviated edema of the widened pancreatic islet exocrine interface in T1DM mice. We conclude that insulin protects against T1DM-induced ultrastructural abnormalities of the pancreatic islet microcirculation.

**Key words:** pancreatic islet microcirculation, ultrastructure, type 1 diabetes mellitus, endothelial cell, pericyte, insulin

## Introduction

Type 1 diabetes mellitus (T1DM) is a chronic metabolic disease characterized by hyperglycemia and autoimmune antibodies that destroy insulin-secreting pancreatic  $\beta$  cells. According to the estimate of the Type 1 Diabetes China Study Group, the incidence of T1DM in China across all age groups combined is 1.01 per 100 000 person-years [1, 2]. Although the pathophysiological basis of T1DM remains to be clarified, recent findings have suggested that the disturbance of

pancreatic islet microcirculation can contribute to the pathogenesis and development of diabetes [3–5]. Pancreatic islet microcirculation, which matches the metabolic supply to the physiological demand of the islet, entails dynamic adjustment of pancreatic islet microvessels by islet microvascular endothelial cells (IMECs) and pericytes (IMPCs). Microcirculatory maladjustment may lead to inadequate nutrient supply in response to glucose variations, causing consequential pancreatic islet dysfunction.

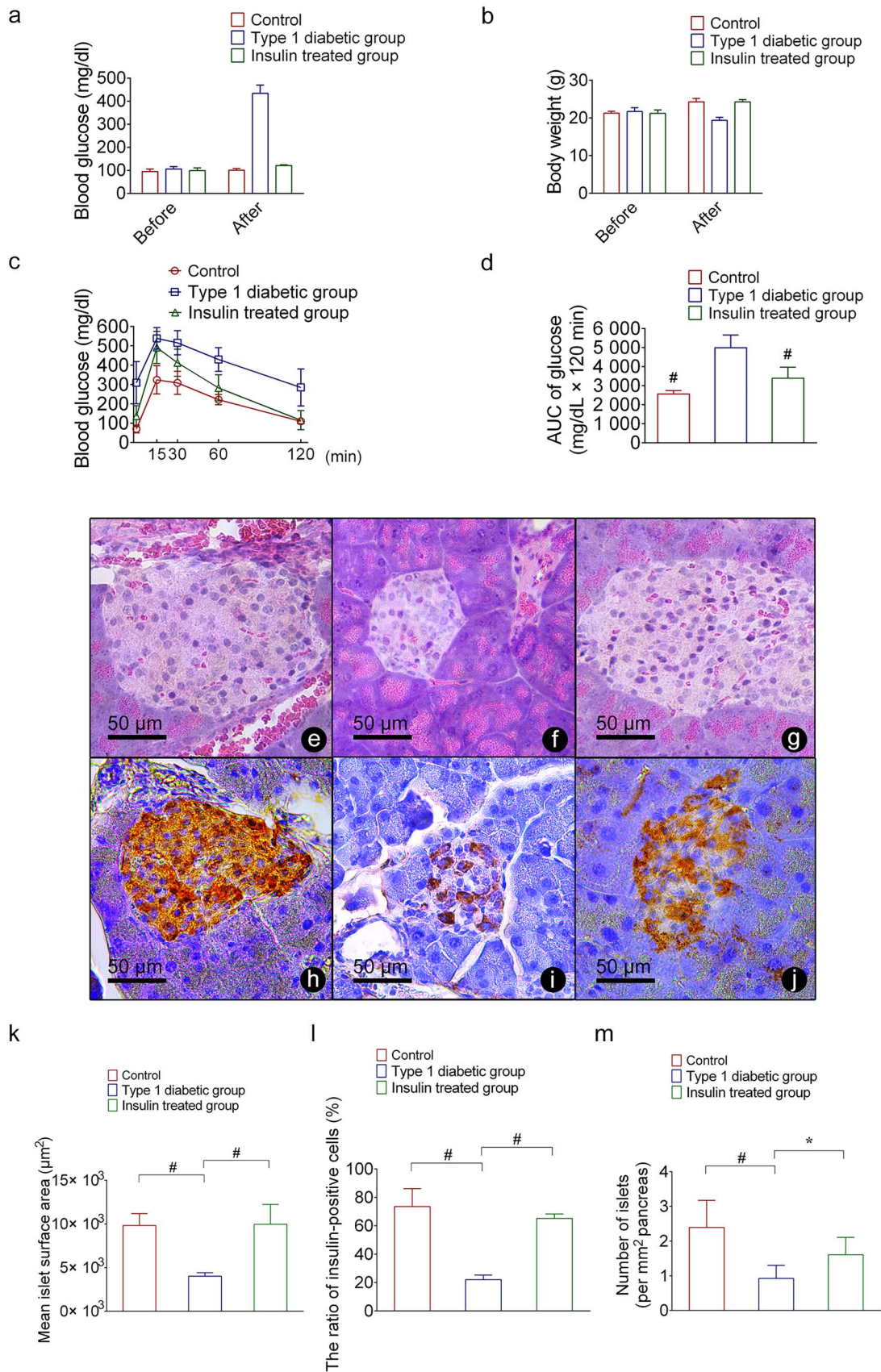


**Fig. 1.** Characterization of the STZ-induced T1DM model. (a) Blood glucose levels in the nondiabetic (control), type 1 diabetic (T1DM) and insulin treated groups. (b) Body weight among the three groups. (c–d) Intraperitoneal glucose tolerance test and AUC<sub>glucose</sub>. Type 1 diabetic mice significantly impaired glucose tolerance

Insulin-secreting pancreatic islets are distributed in highly vascularized pancreatic islet microcirculation [6, 7]. Each islet is adjacent to microvessels to allow direct interaction with fenestrated pancreatic IMECs, which facilitate precise sensing of blood glucose fluctuation and secreting hormones including insulin into the bloodstream according to metabolic demands. Furthermore, IMPCs have been demonstrated to participate in promoting insulin synthesis by regulating  $\beta$  cell maturity and pancreatic islet blood flow [7–10]. Therefore, the structural and functional integrity of the pancreatic islet microcirculation is of importance to physiological islet  $\beta$  cell function.

Dissecting the ultrastructure of the pancreatic islet microcirculation is the key challenge in confirming the link between the original theory of T1DM and the crucial role of pancreatic islet microcirculation. Decreased microcirculatory blood perfusion of the pancreatic islets might be an explanation for the malfunction of islet  $\beta$  cells in T1DM in our previous work [11]. Additionally, several studies have shown that IMECs and IMPCs [12, 13], together with impaired islet  $\beta$  cells [14, 15], might be associated with T1DM occurrence and progression. It is well established that insulin dramatically alters the outcomes of T1DM patients by protecting the function of residual islet  $\beta$  cells. However, if we shift the focus from the islets of Langerhans to the islet microcirculatory niche, the situation will be quite interesting. To the best of our knowledge, few studies have investigated the protective role of insulin against T1DM-induced ultrastructural abnormalities of the pancreatic islet microcirculation. The aim of the current study, therefore was to investigate whether insulin treatment could alleviate the pathological ultrastructural alterations of the pancreatic islet microcirculation in T1DM.

## Materials and methods

### Animals

This study was approved by the Institutional Animal Care and Use Committee (IACUC) at the Chinese Academy of Medical Science (CAMS) and all experiments were performed in accordance with the Guidelines for the Care and Use of Laboratory Animals (No. IACUC-201709). Specific-pathogen-free male BALB/c mice, provided by the Institute of Laboratory Animal Science (CAMS, Beijing, China), were bred and housed at  $22 \pm 1^\circ\text{C}$  with 55–65% humidity and a 12 h: 12 h light: dark cycle. All mice were given standard laboratory diet with free access to water.

### Type 1 diabetic mouse model

Eighteen BALB/c mice were divided into control, type 1 diabetic and insulin-treated groups ( $n = 6$  per group). To induce the type 1 diabetic model, 40 mg/kg streptozotocin (STZ; Sigma-Aldrich, MO, USA) was administered intraperitoneally to the type 1 diabetic group for 5 consecutive days, whereas control mice were given the same volume of sodium citrate buffer. Blood glucose was measured with a glucometer (One Touch UltraEasy, Johnson and Johnson, CA,

USA) 2 weeks after STZ injection. Mice with blood glucose levels  $>200$  mg/dl were considered diabetic. In order to maintain the blood glucose of the insulin-treated group within the normal range, 1–1.5 IU/day insulin was injected *s.c.*

### Intraperitoneal glucose tolerance test

In order to evaluate pancreatic islet function and the capacity to regulate blood glucose, an intraperitoneal glucose tolerance test (IPGTT) was performed. Briefly, after fasting overnight, mice were injected with 2 g/kg D-glucose solution intraperitoneally. Blood samples were collected from the tail vein before and 15, 30, 60 and 120 min after glucose administration. The blood glucose level was measured using a glucometer (Johnson and Johnson). The area under the glucose curve ( $\text{AUC}_{\text{glucose}}$ ) was calculated and compared among the three groups of mice.

### Hematoxylin–eosin staining and immunohistochemistry

Hematoxylin–eosin (HE) staining was applied to evaluate histopathologic changes in the pancreatic islet microcirculation. Pancreatic tissues were fixed in 4% paraformaldehyde and embedded in paraffin. Sections (5  $\mu\text{m}$ ) were subjected to HE staining as well as immunohistochemical staining. Antigen retrieval was performed with 10 mM citrate buffer (pH 6.0, Zhongshan Golden Bridge Biotechnology, Beijing, China). Immunostaining for insulin was then performed as previously reported [16]. Briefly, in order to inhibit endogenous peroxidase, deparaffinized pancreas sections were treated with 3% hydrogen peroxide, followed by blocking with 3% bovine serum albumin (TBD Science Technology, Tianjin, China) in phosphate buffered saline (PBS). Primary mouse monoclonal antibody raised against insulin (2D11-H5) (1: 50; Santa Cruz Biotechnology, Dallas, TX, USA) was incubated in blocking buffer overnight at  $4^\circ\text{C}$ . The same concentration of normal IgG (Santa Cruz Biotechnology) was applied instead of primary antibody as a negative control. After being rinsed, the sections were then incubated with horseradish peroxidase-conjugated secondary antibody (Zhongshan Golden Bridge). After multiple washing steps, the sections were placed in 3,3'-diaminobenzidine tetrahydrochloride solution (Zhongshan Golden Bridge) for 2–10 min, which was monitored on a microscope. Slides were then washed and mounted prior to observation. Positive staining of insulin in pancreatic islets was captured using a Leica DFC450 microscope (Leica Microsystems, Leitz, Germany).

### Pancreatic islet morphometric analysis

For further morphometric analysis, the density of scattered islets, the density of insulin-positive  $\beta$  cells and the mean surface area of islets were quantified. The number of islets (per  $\text{mm}^2$  of pancreas) was manually counted for each section. Insulin-positive  $\beta$  cells were counted and expressed as the ratio of insulin-positive  $\beta$  cells per islet using Image-Pro Plus 6.0 (Media Cybernetics, Silver Springs, MD, USA). Likewise, the mean surface area ( $\mu\text{m}^2$ ) of islets was analyzed

---

after glucose administration compared with that of control and insulin treated mice. The area under the glucose curve ( $\text{AUC}_{\text{glucose}}$ ) was calculated by the trapezoidal method to measure the degree of glucose tolerance impairment. The T1DM group had higher  $\text{AUC}_{\text{glucose}}$  values than the other two groups. (e–g) HE staining of the pancreatic islet microcirculation in the control, T1DM and insulin treated groups. Representatives of pancreatic islets and microvasculature are illustrated. Scale bar = 50  $\mu\text{m}$ . (h–j) Immunohistochemical staining of insulin in the three groups. Scale bar = 50  $\mu\text{m}$ . (k) Mean islet surface area (per  $\mu\text{m}^2$ ) of the three groups. (l) The ratio of insulin-positive cells per islet of the three groups. (m) The number of islets per  $\text{mm}^2$  pancreas among the three groups. Data are expressed as the mean  $\pm$  SD ( $n = 6$  in each group). \* $P < 0.05$  compared with the T1DM group. # $P < 0.01$  compared with the T1DM group.



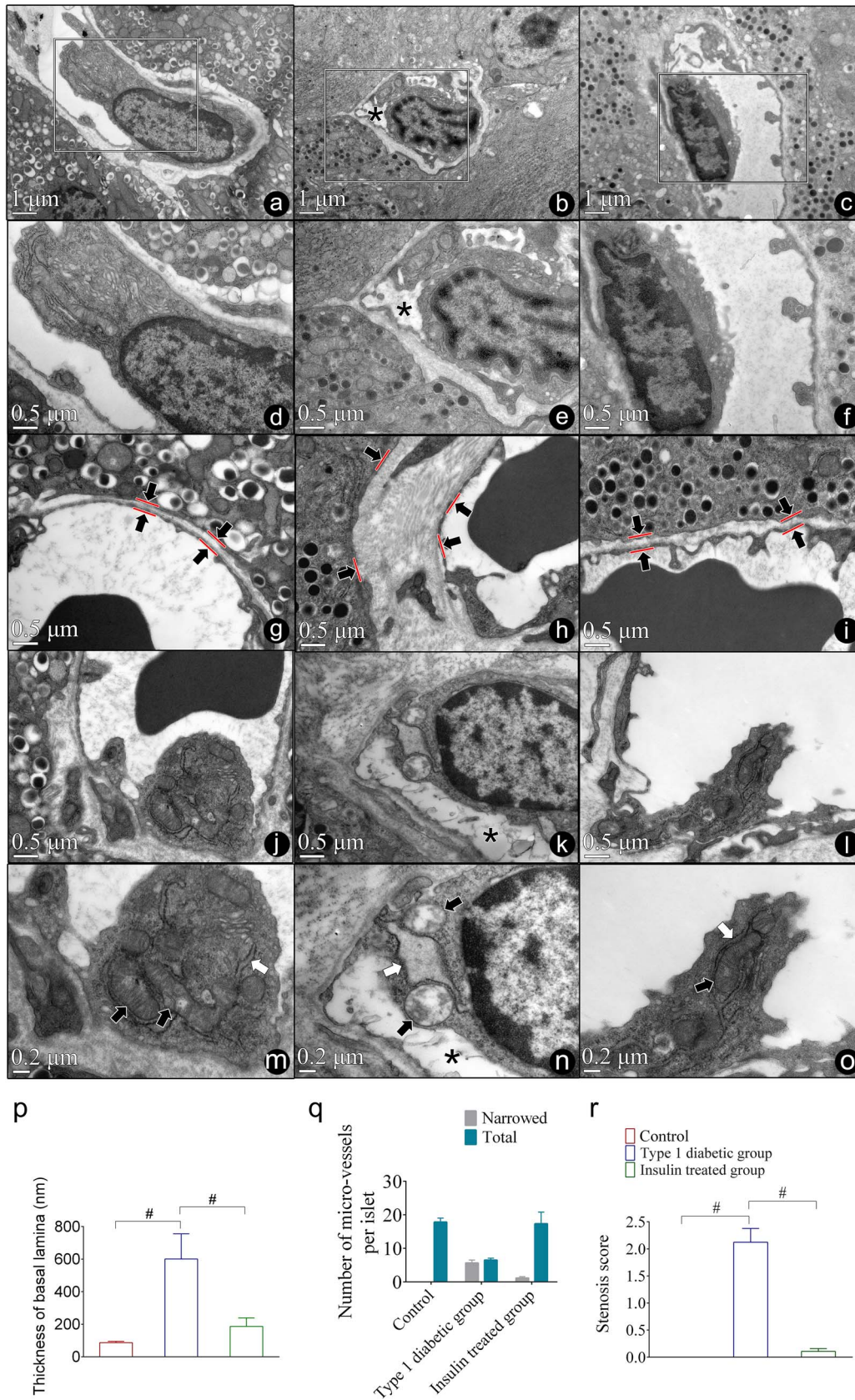


**Fig. 2.** Insulin protects against T1DM-induced pancreatic IMEC ultrastructural damage. (a–c) Ultrastructure of pancreatic IMECs in the control (a), T1DM (b) and insulin treated (c) groups. IMEC swelling and narrowed microvascular lumen (asterisk) were observed in T1DM mice. Insulin treatment ameliorated the twisted

by using ImageJ software (<https://imagej.nih.gov/ij/>). About 30–50 islets per pancreas of each of the three groups were analyzed in a blinded fashion; all morphometric measurements were performed by the same investigator (X.Z.).

### Transmission electron microscopy

Transmission electron microscopy (TEM) was employed to detect ultrastructural changes in pancreatic islet microcirculation in the control, type 1 diabetic and insulin-treated groups. Fresh pancreatic tissues were fixed in 3% buffered glutaraldehyde for 3 h and 1% (w/v) osmic acid for 1 h, followed by dehydration in a graded acetone series and embedding in Epon812 (SPI, PA, USA). After polymerization of the resin at 60°C for 24 h, ultrathin sections were cut at 70 nm in thickness with ultramicrotome using a diamond knife, stained with 5% uranyl acetate and lead citrate, and observed under a JEM 1230 transmission electron microscope (JEOL Co., Ltd, Japan). The ultrastructure of the pancreatic islet microcirculation, including pancreatic IMECs, IMPCs and islet exocrine interface (IEI) of the control, type 1 diabetic and insulin-treated groups, was evaluated.

### Assessment of microvascular occlusion

In order to further investigate pancreatic islet microvascular occlusion, the thickness of the basement membrane of IMECs and the ratio and degree of microvascular narrowing were quantified. All capillaries in each selected islet were scored and semiquantitatively analyzed to evaluate the degree of microvascular narrowing. Each capillary was scored as follows: 0, open lumen and no swelling of endothelial cells; 1, endothelial cell swelling and thickening or distortion of basement membrane, with up to 25% narrowing of lumens in affected capillaries; 2, moderate to severe endothelial cell swelling and thickening or distortion of basement membrane, with 25–50% narrowing of lumens in affected capillaries; 3, severe endothelial cell swelling and thickening or distortion of basement membrane, with >50% narrowing of lumens of capillaries.

### Pancreatic IMEC culture

The pancreatic IMEC cell line (MS1) was purchased from the American Type Culture Collection (ATCC, Manassas, VA, USA). IMECs were seeded in 25 cm<sup>2</sup> cell culture flasks in Dulbecco's modified Eagle's medium (DMEM, Gibco, Carlsbad, CA, USA), supplemented with 5.6 mM glucose, 10% fetal bovine serum (FBS, Bovogen Biologicals, VIC, AUS), 4 mM L-glutamine, and penicillin (100 U/ml)/streptomycin (100 µg/ml). Pancreatic IMECs derived from the same passage were employed in all experiments to make the data comparable among groups. After IMECs (passage 4) were confluent, cells were divided into control (5.6 mM glucose), diabetic (35 mM glucose) and insulin-treated (35 mM glucose +10<sup>-8</sup> M

insulin) groups and were received their respective treatments for 48 h respectively ( $n = 3$  each group).

### Scanning electron microscopy

In order to detect the ultramorphology of the pancreatic IMEC surface alone or affected by insulin against glucose toxicity, IMEC samples were prepared for scanning electron microscopy (SEM) by adding freshly prepared fixative buffer (1% glutaraldehyde in 0.1 M sodium cacodylate buffer) to the cell slides overnight at 4°C. After being rinsed in 0.1 M PBS, samples were postfixed in 1% osmium tetroxide for 2 h. They were then dehydrated in a graded acetone series, followed by tert-butanol and freeze dried using a freeze vacuum dryer (ES-2030, Hitachi, Japan). After being glued onto SEM stubs, samples were sputter coated with a 10 nm thick layer of gold for 60 s to further enhance conductivity (E-1010, Hitachi, Japan) and observed using a scanning electron microscope (S-3400 N, Hitachi, Japan) under high-vacuum mode at 5 kV.

### Statistical analysis

All data are expressed as the mean ± standard deviation. Statistical analysis was performed by Statistical Package for the Social Sciences (SPSS, version 19.0, Chicago, IL, USA). Comparisons of the pancreatic islet microcirculation in different groups were conducted by independent-sample *t*-tests. A *P* value less than 0.05 was considered statistically significant.

## Results

### Characterization of the STZ-induced T1DM mouse model

We first sought to characterize the T1DM mouse model induced by STZ injection. The blood glucose and body weight of the three groups of mice were shown in Fig. 1. No significant differences in either blood glucose or body weight at baseline were found among the three groups (Fig. 1a and b). The blood glucose level was noted to be significantly higher in type 1 diabetic mice than that in the control or insulin-treated group, and the body weight of the diabetic group was significantly lower than that in the control or insulin-treated mice. As shown in Figure 1c and d, IPGTT data demonstrated that there was a significantly impaired glucose tolerance and a higher AUC<sub>glucose</sub> in type 1 diabetic mice following glucose administration compared with those of the control and insulin-treated groups. Furthermore, HE images and immunohistochemistry labeling of insulin in pancreatic tissue revealed decreased islet size and density of islet microvessels (Fig. 1e–g) as well as a reduced number of insulin-positive cells in islets (Fig. 1h–j), suggesting morphological abnormalities in the diabetic pancreatic islet microcirculation. In addition, quantitative analysis revealed that T1DM mice had a significantly smaller islet sur-

lumen. Scale bar = 1 µm. (d–f) The inserts in (a–c) are magnified. (d) Control IMECs. (e) IMECs in type 1 diabetic mice. The asterisk indicates a narrowed capillary lumen. (f) Insulin treated IMECs. Scale bar = 0.5 µm. (g–i) Capillary basement membrane (arrows) in the control (g), T1DM (h) and insulin treated (i) groups. Scale bar = 0.5 µm. (j–l) Organelles of IMECs in the control (j), T1DM (k) and insulin treated (l) groups. The asterisk indicates a narrowed capillary lumen. Scale bar = 0.5 µm. (m–o) Organelles in (j–l) are magnified. (m) Mitochondria (black arrows) and rough endoplasmic reticulum (RER) (white arrow) in the control group. (n) Swollen mitochondria with cristae rupture and disappeared matrix (black arrows) and dilated RER (white arrow) in T1DM mice. The asterisk indicates a narrowed capillary lumen. (o) Restored mitochondrion (black arrow) and RER (white arrow) after insulin administration. Scale bar = 0.2 µm. (p) Thickness of the basal lamina of the control, T1DM and insulin treated groups. (q) The number of pancreatic islet microvessels per islet. The gray column represents the number of narrowed microvessels. The blue column represents the total number of microvessels. (r) The degree of pancreatic islet microvascular narrowing in the control, T1DM and insulin treated groups was assessed by stenosis score. Data are expressed as the mean ± SD ( $n = 6$  in each group). #*P* < 0.01 compared with the T1DM group.



face area than control ( $P < 0.01$ ) and insulin-treated mice ( $P < 0.01$ ) (Fig. 1k). The ratio of insulin-positive cells (Fig. 1l) and the number of islets per millimeter square pancreas were lower in T1DM mice, and the differences were statistically significant compared with control ( $P < 0.01$ ) and insulin-treated mice ( $P < 0.05$ ) (Fig. 1m). Taken together, these findings suggested that the T1DM mouse model was successfully established by injecting 40 mg/kg STZ consecutively.

### Insulin protects pancreatic IMECs against ultrastructural damage induced by T1DM

TEM observation revealed IMECs with normal architecture resting on a thin basal lamina in the control group (Fig. 2a, d and g). Control IMECs exhibited ovoid nuclei and well-arranged rough endoplasmic reticulum (RER) and mitochondria scattered in the cytoplasm (Fig. 2j and m). In contrast, T1DM mice displayed narrowed or closed lumens (Fig. 2b and e) with contorted and thickened basement membranes (Fig. 2h), and swollen IMECs with mitochondrial swelling and RER distention (Fig. 2k and n), suggesting that the ultrastructure of pancreatic IMECs was impaired in the T1DM group. IMECs of the insulin-treated group demonstrated a wide capillary lumen and thin basement membrane (Fig. 2c, f and i). Meanwhile, the mitochondria and RER were restored to normal in insulin-treated IMECs (Fig. 2l and o). Quantitative analysis revealed that T1DM mice showed a significantly thicker basement membrane than control ( $P < 0.01$ ) or insulin-treated mice ( $P < 0.01$ ) (Fig. 2p). Furthermore, insulin-treated mice exhibited a decreased ratio (6.73 vs 87.18% in T1DM) of narrowed microvessels ( $P < 0.01$ ) (Fig. 2q), with a significantly lower stenosis score ( $P < 0.01$ ) (Fig. 2r) than the T1DM group. These improvements in microvascular ultrastructural pathology may be attributable to the protective role of insulin treatment.

We then employed SEM to investigate whether insulin would improve the ability of IMECs to maintain endothelial integrity. To this end, we prepared a pancreatic-derived IMEC cell line (MS1) and incubated the IMECs with glucose or insulin *in vitro*. SEM images demonstrated that insulin treatment was beneficial for IMEC viability (Fig. 3). IMECs in the control group exhibited smooth surfaces covered with abundant microvilli (Fig. 3a). In contrast, incubation with a high concentration of glucose destroyed the integrity of IMECs, causing them to have rough surfaces with no microvilli (Fig. 3b). After insulin administration, IMECs displayed a completely stretched contour with short microvilli and blebs on the surface, similar to normal epithelial cells (Fig. 3c). These data suggested that insulin effectively ameliorated the ultrastructural abnormalities of IMECs resulting from glucose toxicity.

### Insulin protects pancreatic IMPC ultrastructural damage induced by T1DM

As for pancreatic IMPCs, ultrastructural evaluation revealed that IMPCs of control (Fig. 4a and d) and insulin-treated mice (Fig. 4c and f) had elongated longitudinal and thin cytoplasmic foot processes enveloping to IMECs. In contrast, the shape of IMPCs in diabetic mice became irregular with foot process loss (Fig. 4b and e). The nuclei of diabetic IMPCs lost elliptical shape and exhibited irregular ultramorphology, compared with control and insulin-treated mice. However, no intergroup difference was found in the number of IMPCs in intraislet capillaries (data not shown). As in IMECs, injury of cellular organelles, such as swollen mitochondria

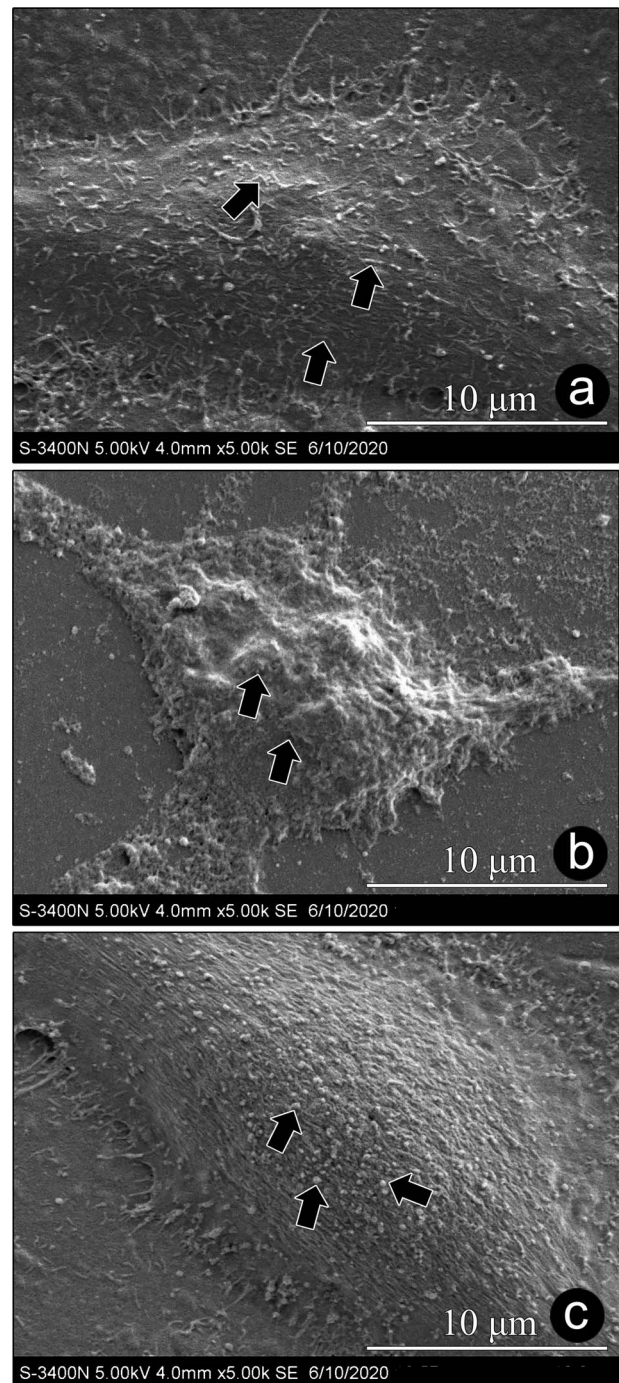


**Fig. 3.** Insulin protects against glucose toxicity-induced pancreatic IMEC ultrastructural damage. SEM images of IMECs were obtained from MS1 *in vitro*. (a) Control group. The arrows indicate enriched microvilli on the IMEC surface. (b) Diabetic group (35 mM glucose). The arrows indicate disrupted integrity of IMECs with rough surfaces and disappeared microvilli. (c) Insulin-treated group (35 mM glucose +  $10^{-8}$  M insulin). The arrows indicate blebs on the smooth surface of IMEC. Scale bar = 10  $\mu$ m.

and dilated RER, could also be observed in IMPCs of the type 1 diabetic group. The mitochondria were enlarged and had decreased matrix density and ruptured cristae (Fig. 4e and h). Additionally, as observed in control mice (Fig. 4d and g), IMPCs were restored to

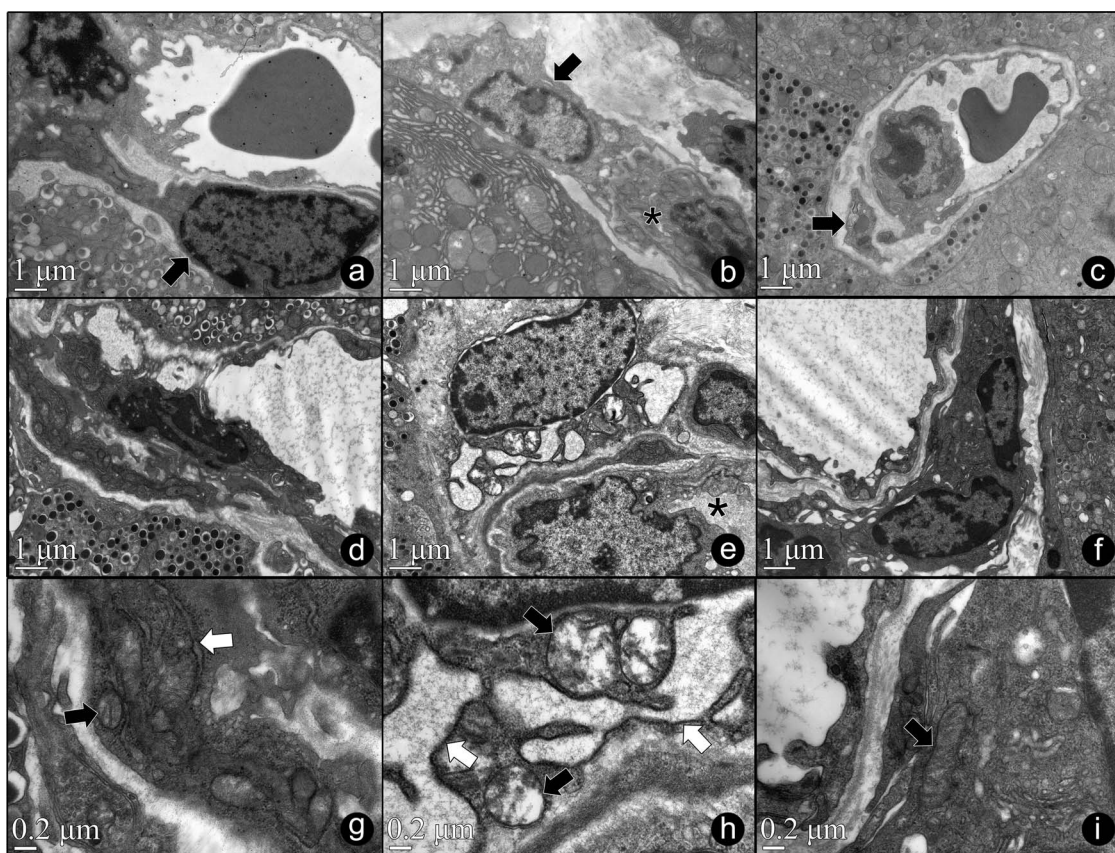


**Fig. 4.** Insulin protects against T1DM-induced pancreatic IMPC ultrastructural damage. (a–c) Representative TEM images of IMPCs obtained from the control (a), T1DM (b) and insulin treated (c) groups. The shape of IMPC became irregular in T1DM mice. The asterisk indicates an occlusive capillary lumen. Scale bar = 1  $\mu\text{m}$ . (d–f) Organelles of pancreatic IMPCs in the control (d), type 1 diabetic (e) and insulin treated (f) groups. The asterisk indicates an occlusive capillary lumen. Scale bar = 1  $\mu\text{m}$ . (g–i) Organelles in (d–f) are magnified. (g) Normal mitochondrion (black arrow) and RER (white arrow) of control IMPCs. (h) Swollen mitochondria (black arrows) and dilate RER (white arrows) in diabetic mice. (i) Insulin treatment restored the ultramorphology of organelles of IMPCs. The arrow indicates a restored mitochondrion. Scale bar = 0.2  $\mu\text{m}$ .

regular shapes, and the morphology of mitochondria was normal with characteristic arranged cristae in the insulin-treated group (Fig. 4f and i).

#### Insulin reverses T1DM-induced pancreatic IEC destruction

The normal IEC is a tight interface between a pancreatic islet and the surrounding exocrine tissue (Fig. 5a). The IEC in the type 1 diabetic mice mostly lost its normal structure, especially those adjacent to the pancreatic islet microvessels and small arteries (Fig. 5b and c). The IEC was noticeably widened, with collagenous fibrils proliferating around peri-islet pericytes and peri-islet endothelial cells, which deteriorated the intercommunication within the pancreatic islet microcirculation of type 1 diabetic mice (Fig. 5b). Furthermore, banded fibrillar collagen penetrated into the area between exocrine and pancreatic islet  $\beta$  cells with marked edema (Fig. 5c), which was not observed in the pancreatic microcirculation of control mice. The mean width of the IEC in the T1DM group was significantly higher than that in the control ( $P < 0.01$ ) or insulin-treated mice ( $P < 0.01$ ). Treatment of type 1 diabetic mice with insulin completely protected the IEC architecture against pathological alterations secondary to T1DM (Fig. 5d and e).

#### Discussion

The current study provides evidence that insulin treatment alleviates the deteriorated ultrastructure of pancreatic IMECs and IMPCs in T1DM mouse model, which substantially protects the pancreatic islet microcirculation. Pancreatic islet microcirculation is a novel concept of great potential significance, particularly within the realm of diabetes mellitus in humans and animals [14, 15, 17, 18]. In our previous study, we demonstrated that the pancreatic islet microcirculation lost the ability to adjust pancreatic islet microcirculatory blood distribution in STZ-induced T1DM mice. In order to regulate glucose metabolic homeostasis, integrated pancreatic islet microcirculation is necessary for insulin transportation. As the component cells of pancreatic islet microcirculation, IMECs and IMPCs therefore participate in supporting the proper function of insulin-secreting  $\beta$  cells and regulating blood glucose fluctuation [8]. In our data, we observed ultrastructural damage to these two crucial pancreatic microcirculatory component cells after T1DM induction.

IMECs, as the functional units of the pancreatic islet microcirculation, play a vital role in glucose homeostasis [12]. Structural and functional injury of pancreatic IMECs caused by T1DM is increasingly considered to be the result of glucose toxicity and pancreatic islet inflammation. Furthermore, poor glycemic administration activates inflammatory cytokines [19–21], which may lead to deterioration of



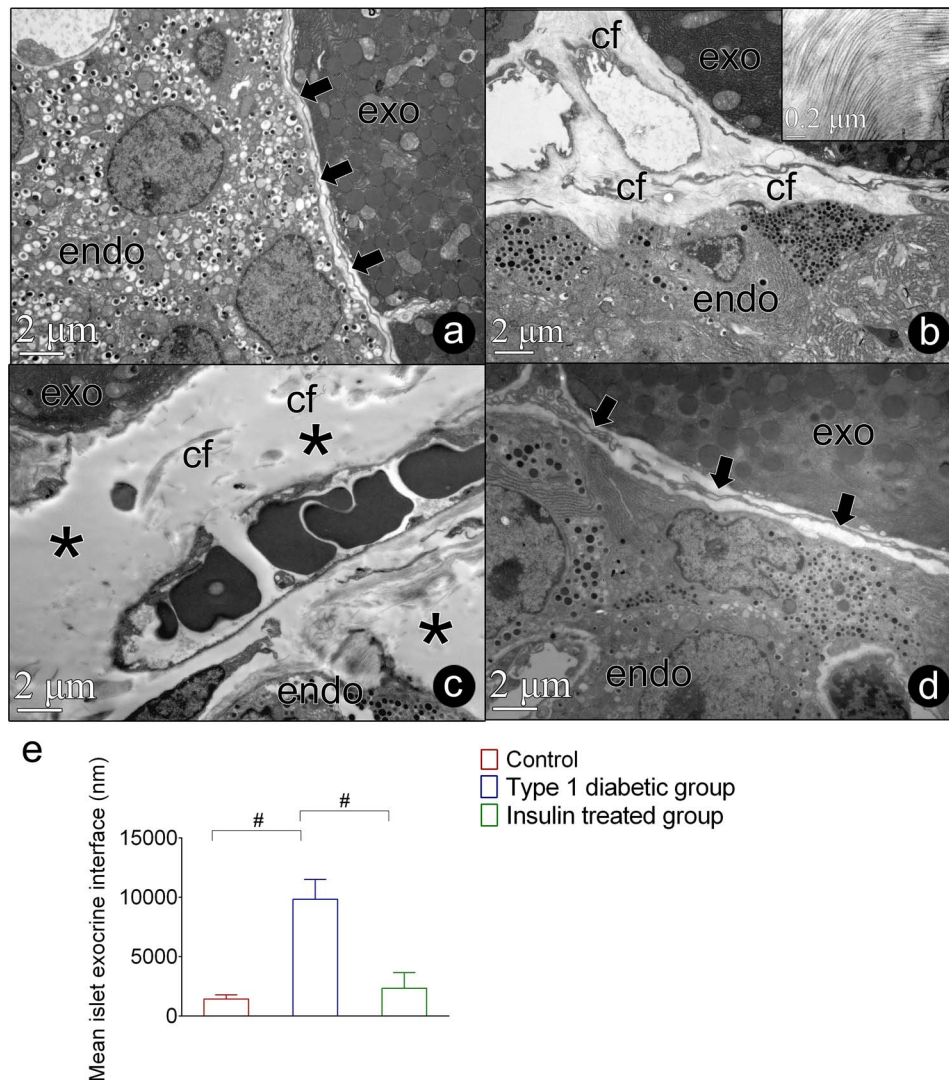


**Fig. 5.** Insulin restores damaged IEI induced by T1DM. (a) IEI (arrows) of control mice. (b) Proliferative collagenous fibers (cf) intruded into the IEI in T1DM mice. The insert shows representative proliferative collagenous fibers at higher magnification. (c) Collagenous fibers (cf) penetrated into the edema area (asterisks) between the exocrine and endocrine portions in T1DM mice. (d) IEI of the insulin treated group (arrows). (e) The width of the mean islet exocrine interface of the control, T1DM and insulin treated groups. Data are expressed as the mean  $\pm$  SD ( $n = 6$  in each group). # $P < 0.01$  compared with the T1DM group. Scale bar = 2  $\mu$ m in the main ultrastructural graph and scale bar = 0.2  $\mu$ m in the insert. Endo, endocrine; Exo, exocrine.

pancreatic islet microcirculation. Our observations of the damaged ultrastructure of IMECs are in agreement with the above findings. The antihyperglycemic and anti-inflammatory effects of insulin could be one of the explanations for microcirculatory ultrastructural protection and restoration. Moreover, alterations in mitochondrial ultrastructure have been described in various pathological conditions, including T1DM. Defect mitochondrial function has been speculated to correlate with inadequate adenosine triphosphate generation that fails to meet the metabolic demand for adjustment of pancreatic islet microcirculation. We found that, in the presence of insulin treatment, the disarranged and swollen mitochondria of IMECs in type 1 diabetic mice were restored, causing an increased microcirculatory exchange surface area and microvascular blood perfusion [22, 23]. Therefore, insulin treatment protects IMECs against ultramorphological damage, helping maintain the structural integrity of the pancreatic islet microcirculation.

It has been previously suggested that, as an essential cellular component of the pancreatic islet microcirculation, pancreatic IMPCs are responsible for microcirculatory blood flow perfusion by adjusting microvessel diameter [24]. Pancreatic IMPCs are specialized microcirculatory cells that play an important role in collagen fiber synthesis, angiogenesis and maintenance of microvascular permeability [24–26]. Additionally, pancreatic IMPCs are vulnerable to metabolic oxidative-redox stress and toxicity derived from T1DM [27]. In this regard, our observation of ultrastructural impairment of IMPCs in T1DM emphasizes the importance of pancreatic islet microcirculation. Furthermore, our data indicate that insulin could reverse the pathological ultrastructural alterations of IMPCs.

On the other hand, because microvascular pericytes and endothelial cells share the same basement membrane [28], there might be an interaction between IMECs and IMPCs through closely apposed foot processes, peg sockets and adherent junctions. In the current



study, unlike loss of pericyte foot processes in T1DM mice, longitudinal elongated IMPCs and enveloped cytoplasmic foot processes were observed in control and insulin-treated mice. Interestingly, a crosstalk within the pancreatic islet microcirculation, where the cellular foot processes of pancreatic IMECs, IMPCs and  $\beta$  cells meet, was visualized in the control and insulin-treated groups (please see [Supplementary Fig. S1](#)). These lines of evidence confirm the protective role of insulin against T1DM-induced ultrastructural abnormalities.

The IEI is considered a crucial structural and functional region in the pancreatic islet microcirculation [29, 30], which is essential for insulin secretion and communication between  $\beta$  cells and pancreatic islet microcirculatory components. Normally, the IEI is responsible for keeping the pancreatic exocrine and islets in close anatomical adjacency. Widening of the IEI interferes with efferent and afferent transportation of insulin, and even delays first phase insulin secretion in diabetic patients [31]. The TEM data revealed that the IEI became fibrotic and considerably widened in T1DM mice, resulting in inadequate or entirely absent crosstalk between the interrelated subdivisions of the pancreatic islet microcirculation. Furthermore, the protective role of insulin in alleviating fibrogenesis and edema in IEI of insulin-treated T1DM mice might be associated with fibrous synthesis suppression [32] and the anti-inflammatory activity of insulin [33]. Collectively, our data indicate an ultrastructural stabilization effect of insulin on the pancreatic islet microcirculation.

## Concluding remarks

In the current study, we provide a comprehensive description and ultrastructural evidence explaining how induction of T1DM results in damage to pancreatic IMECs, IMPCs and the IEL, while insulin treatment can protect against ultrastructural abnormalities of the pancreatic islet microcirculation. These observations may offer an opportunity for new insights into the understanding of pancreatic islet microcirculation in T1DM.

## Supplementary data

[Supplementary data](#) are available at *JMICRO* online.

## Conflict of interest statement

The authors declare that they have no conflict of interest.

## Funding

Chinese Academy of Medical Science Initiative for Innovative Medicine (2016-I2M-3-006 to H.G.Z.) and the National Natural Science Foundation of China (81900747 to M.M.L.).

## Acknowledgements

The authors are most grateful for Prof. Suxia Wang and Jin Xu (chief technician) at Peking University First Hospital, Laboratory of Electron Microscopy for their excellent TEM and SEM technical assistance.

## References

- Xu Y, Wang L, He J, Bi Y, Li M, Wang T, Wang L, Jiang Y, Dai M, Lu J, Xu M, Li Y, Hu N, Li J, Mi S, Chen C S, Li G, Mu Y, Zhao J, Kong L, Chen J, Lai S, Wang W, Zhao W, and Ning G (2013) Prevalence and control of diabetes in Chinese adults. *JAMA* 310: 948–959.
- Weng J, Zhou Z, Guo L, Zhu D, Ji L, Luo X, Mu Y, and Jia W (2018) Incidence of type 1 diabetes in China, 2010–13: population based study. *BMJ* 360: j5295.
- Amarteifio E, Wormsbecher S, Demirel S, Krix M, Braun S, Rehnitz C, Delorme S, Kauczor H U, and Weber M A (2013) Assessment of skeletal muscle microcirculation in type 2 diabetes mellitus using dynamic contrast-enhanced ultrasound: a pilot study. *Diab. Vasc. Dis. Res.* 10: 468–470.
- Heimhalt-El Hamriti M, Schreiber C, Noerenberg A, Scheffler J, Jacoby U, Haffner D, and Fischer D C (2013) Impaired skin microcirculation in paediatric patients with type 1 diabetes mellitus. *Cardiovasc. Diabetol.* 12: 115.
- Wiernsperger N, Nivoit P, De Aguiar L G, and Bouskela E (2007) Microcirculation and the metabolic syndrome. *Microcirculation* 14: 403–438.
- Ballian N, and Brunicaudi F C (2007) Islet vasculature as a regulator of endocrine pancreas function. *World J. Surg.* 31: 705–714.
- Reinert R B, Brissova M, Shostak A, Pan F C, Poffenberger G, Cai Q, Hundemer G L, Kantz J, Thompson C S, Dai C, McGuinness O P, and Powers A C (2013) Vascular endothelial growth factor- $\alpha$  and islet vascularization are necessary in developing, but not adult, pancreatic islets. *Diabetes* 62: 4154–4164.
- Sasson A, Rachi E, Sakhneny L, Baer D, Lisnyansky M, Epshtein A, and Landsman L (2016) Islet pericytes are required for beta-cell maturity. *Diabetes* 65: 3008–3014.
- Kim J, Kim C S, Sohn E, Lee Y M, Jo K, and Kim J S (2012) KIOM-79 protects AGE-induced retinal pericyte apoptosis via inhibition of NF- $\kappa$ B activation in vitro and in vivo. *PLoS One* 7: e43591.
- Gerhardt H, and Betsholtz C (2003) Endothelial-pericyte interactions in angiogenesis. *Cell Tissue Res.* 314: 15–23.
- Liu M, Zhang X, Li A, Zhang X, Wang B, Li B, Liu S, Li H, and Xiu R (2017) Insulin treatment restores islet microvascular vasomotion function in diabetic mice. *J. Diabetes* 9: 958–971.
- Zanone M M, Favaro E, and Camussi G (2008) From endothelial to beta cells: insights into pancreatic islet microendothelium. *Curr. Diabetes Rev.* 4: 1–9.
- Ejaz S, Chekarova I, Ejaz A, Sohail A, and Lim C W (2008) Importance of pericytes and mechanisms of pericyte loss during diabetes retinopathy. *Diabetes Obes. Metab.* 10: 53–63.
- Hayden M R, Karuparthi P R, Habibi J, Lastra G, Patel K, Wasekar C, Manrique C M, Ozerdem U, Stas S, and Sowers J R (2008) Ultrastructure of islet microcirculation, pericytes and the islet exocrine interface in the HIP rat model of diabetes. *Exp. Biol. Med.* 233: 1109–1123.
- Masini M, Martino L, Marselli L, Bugliani M, Boggi U, Filippini F, Marchetti P, and De Tata V (2017) Ultrastructural alterations of pancreatic beta cells in human diabetes mellitus. *Diabetes Metab. Res.* 33: e2894.
- Zimmermann C, Cederroth C R, Bourgoin L, Foti M, and Nef S (2012) Prevention of diabetes in db/db mice by dietary soy is independent of isoflavone levels. *Endocrinology* 153: 5200–5211.
- Hayden M R, Karuparthi P R, Habibi J, Wasekar C, Lastra G, Manrique C, Stas S, and Sowers J R (2007) Ultrastructural islet study of early fibrosis in the Ren2 rat model of hypertension. Emerging role of the islet pancreatic pericyte-stellate cell. *JOP* 8: 725–738.
- Nordquist L, and Palm F (2007) Diabetes-induced alterations in renal medullary microcirculation and metabolism. *Curr. Diabetes Rev.* 3: 53–65.
- Lozanoska-Ochser B, Klein N J, Huang G C, Alvarez R A, and Peakman M (2008) Expression of CD86 on human islet endothelial cells facilitates T cell adhesion and migration. *J. Immunol.* 181: 6109–6116.
- Gaengel K, Genove G, Armulik A, and Betsholtz C (2009) Endothelial-mural cell signaling in vascular development and angiogenesis. *Arterioscler. Thromb. Vasc. Biol.* 29: 630–638.
- Akirav E M, Baquero M T, Opere-Addo L W, Akirav M, Galvan E, Kushner J A, Rimm D L, and Herold K C (2011) Glucose and inflammation control islet vascular density and beta-cell function in NOD mice: control of islet vasculature and vascular endothelial growth factor by glucose. *Diabetes* 60: 876–883.

22. Staels W, Heremans Y, Heimberg H, and De Leu N (2019) VEGF-A and blood vessels: a beta cell perspective. *Diabetologia* 62: 1961–1968.
23. Townsend S E, and Gannon M (2019) Extracellular matrix-associated factors play critical roles in regulating pancreatic beta-cell proliferation and survival. *Endocrinology* 160: 1885–1894.
24. Almaca J, Weitz J, Rodriguez-Diaz R, Pereira E, and Caicedo A (2018) The pericyte of the pancreatic islet regulates capillary diameter and local blood flow. *Cell Metab.* 27: 630–644.
25. Tang S C, Jessup C F, and Campbell-Thompson M (2018) The role of accessory cells in islet homeostasis. *Curr. Diab. Rep.* 18: 117.
26. Fadini G P, Albiero M, Bonora B M, and Avogaro A (2019) Angiogenic abnormalities in diabetes mellitus: mechanistic and clinical aspects. *J. Clin. Endocrinol. Metab.* 104: 5431–5444.
27. Landsman L (2019) Pancreatic pericytes in glucose homeostasis and diabetes. *Adv. Exp. Med. Biol.* 1122: 27–40.
28. Mandarino L J, Sundarraj N, Finlayson J, and Hassell H R (1993) Regulation of fibronectin and laminin synthesis by retinal capillary endothelial cells and pericytes in vitro. *Exp. Eye Res.* 57: 609–621.
29. Hayden M R, Patel K, Habibi J, Gupta D, Tekwani S S, Whaley-Connell A, and Sowers J R (2008) Attenuation of endocrine-exocrine pancreatic communication in type 2 diabetes: Pancreatic extracellular matrix ultrastructural abnormalities. *J. Cardiometab. Syndr.* 3: 234–243.
30. Hayden M R, and Sowers J R (2007) Isletopathy in type 2 diabetes mellitus: implications of islet RAS, islet fibrosis, islet amyloid, remodeling, and oxidative stress. *Antioxid. Redox Signal.* 9: 891–910.
31. Hayden M R (2007) Islet amyloid and fibrosis in the cardiometabolic syndrome and type 2 diabetes mellitus. *J. Cardiometab. Syndr.* 2: 70–75.
32. Greenhill C (2019) Insulin and the insulin receptor regulate gene expression. *Nat. Rev. Endocrinol.* 15: 315.
33. Zhu Z, Hu T, Wang Z, Wang J, Liu R, Yang Q, Zhang X, and Xiong Y (2018) Anti-inflammatory and organ protective effect of insulin in scalded MODS rats without controlling hyperglycemia. *Am. J. Emerg. Med.* 36: 202–207.